KRT7 promotes epithelial-mesenchymal transition in ovarian cancer via the TGF-β/Smad2/3 signaling pathway

QIANG AN, TING LIU, MING-YANG WANG, YU-JIA YANG, ZHEN-DONG ZHANG, ZHEN-JIANG LIU and BING YANG

Department of Gynecology, Affiliated Hospital of Zunyi Medical University, Zunyi, Guizhou 563000, P.R. China

Received August 20, 2019; Accepted September 24, 2020

DOI: 10.3892/or.2020.7886

Abstract. Keratin 7 (KRT7) is a member of the keratin gene family. KRT7 is abnormally expressed in various types of cancer and promotes the malignant progression of tumors. However, the role of KRT7 in ovarian cancer remains unclear. The present study aimed to validate the role of KRT7 in ovarian cancer progression. KRT7 expression levels in patients with ovarian cancer were analyzed using data obtained from the Human Protein Atlas and The Cancer Genome Atlas databases. KRT7 mRNA and protein expression levels were upregulated in ovarian cancer tissue compared with normal tissue. KRT7 expression was associated with the grading, staging and poor prognosis of ovarian cancer. The differentially expressed genes affected by KRT7 were primarily enriched in the functions of cell migration, cell adhesion and cell growth. *In vitro* studies, including a CCK8 assay, were used to detect cell proliferation. In addition, wound healing and transwell assays were performed to analyze cell migration. The results demonstrated that KRT7 overexpression was associated with increased proliferation, migration and epithelial-mesenchymal transition (EMT) of ovarian cancer cells, and the migration and EMT of ovarian cancers cells were decreased following knockdown with KRT7 small interfering RNA. *In vivo*, knockdown of KRT7 inhibited tumor growth of ovarian cancer. Furthermore, KRT7 regulated EMT in ovarian cancer via the TGF-β/Smad2/3 pathway, and regulated cell-matrix adhesion through integrin-β1-focal adhesion kinase signaling. These results suggest that KRT7 may be a potential molecular marker for prognosis prediction in patients with ovarian cancer.

Introduction

Ovarian cancer is one of the most lethal types of gynecological cancer. Although surgery and chemotherapy can improve survival, the 5-year survival rate remained low at ~50% in the USA in 2015 (1). Epithelial cancer is the most common type of malignant ovarian tumor, followed by malignant germ cell tumor (2-4). Ovarian cancer is difficult to detect during the early stages due to the small size of the ovary, which is located deep in the pelvic cavity, and patients may not exhibit symptoms or may only vaguely show symptoms when tumor cells invade or spread to other parts of the body (5). Patients with ovarian cancer typically have a poor prognosis due to a lack of signs or screening tests that would facilitate early detection, resulting in a considerable proportion of cases being diagnosed at an advanced stage (6). During epithelial-mesenchymal transition (EMT), epithelial cells can repress their epithelial morphology and acquire motile and invasive properties during tumor progression (7). Surgery combined with chemotherapy is the primary treatment modality for patients with ovarian cancer; however, among patients who undergo surgery for removal of an ovarian epithelial tumor, only ~30% of the tumors are confined to the ovary, and the majority of patients have tumors that have spread to pelvic and abdominal organs, resulting in a low success rate of surgical excision (8). Furthermore, the beneficial effects of maintenance chemotherapy have not been clearly demonstrated (9). Therefore, determining the molecular mechanisms underlying metastasis of ovarian cancer may highlight potential novel therapeutic targets.

Keratin 7 (KRT7) is a member of the keratin gene family, which is subdivided into type I (KRT9-KRT22) and type II (KRT1-KRT8) (10). Type II cytokeratin is composed of alkaline or neutral proteins and is specifically expressed in simple epithelial cells in the lumen of the internal organs and in the ducts and blood vessels of glands (11). KRT7 is abnormally expressed in various types of cancer, such as esophageal squamous cell, cervical and colorectal cancers (12-15). KRT7 also participates in cervical cancer invasion, metastasis and promotes the malignant progression of cancer (16). Several studies have reported an association between KRT7 dysregulation and clinical pathology or prognosis (15,17); however, to the best of our knowledge, the molecular mechanisms involving KRT7 in promoting malignant progression have not been determined. KLK4-7 serve key roles in regulating the expression of their associated genes and proteins in ovarian cancer (18). As a downstream effector, KRT7 may be an important therapeutic target for treatment of ovarian cancer.

Correspondence to: Professor Bing Yang, Department of Gynecology, Affiliated Hospital of Zunyi Medical University, Zunyi, Guizhou 563000, P.R. China
E-mail: yangbing2188@163.com

Key words: keratin 7, ovarian cancer, epithelial-mesenchymal transition, TGF-β pathway

However, the expression and function of KRT7 in ovarian cancer has not been determined, to the best of our knowledge.

The present study validates the role of KRT7 in ovarian cancer progression. By using TCGA database and *in vitro* and *in vivo* experiments, the crucial role of KRT7 in the metastasis and proliferation of ovarian cancer cells has been confirmed. This indicates the role of KRT7 in ovarian cancer and may provide a potential target for cancer therapy.

Materials and methods

Cell culture. In the present study, seven ovarian cancer cell lines (HEY, 59M, COV504, COV413A, DOV13, COV318 and OVCAR433), obtained from Nanjing KeyGen Biotech Co., Ltd., were cultured and maintained. Ovarian cancer cells were cultured in RPMI-1640 medium (Gibco; Thermo Fisher Scientific, Inc.) supplemented with 10% FBS (Thermo Fisher Scientific, Inc.) and 1% penicillin-streptomycin solution (Beyotime Institute of Biotechnology) in a 5% CO_2 humidified incubator at 37˚C.

Plasmid construction and cell transfection. pcDNA3.1-KRT7, pcDNA3.1-TGFβ1 and short hairpin psi-H1-shKRT7 plasmids were synthesized by GeneCopoeia Co., Ltd. Plasmids were transfected into HEY and OVCAR433 cells (1 μg plasmid/10^5 cells) using Lipofectamine® 2000 (Invitrogen; Thermo Fisher Scientific, Inc.). pcDNA3.1 and psi-H1 empty vectors were used as the control. After 24 or 48 h, total RNA and protein were extracted, respectively, and then analyzed using reverse transcription-quantitative PCR (RT-qPCR) and western blotting to determine the transfection efficiency. For stable KRT7-knockdown cells, OVCAR433 cells were transfected with the shKRT7 plasmid (1 μg plasmid/10^5 cells) using Lipofectamine® 2000, and cultured with puromycin at a final concentration of 5 μg/ml for 3 weeks to obtain a stable cell line. The KRT7 shRNA sequences were as follows: shKRT7-top, 5'-AATTCGGAATACCCGGAATGAGATTTCGAAAAATCTCATTCCGGGTATTCCG-3'; and shKRT7-bot, 5'-GATCCGGAATACCCGGAATGAGATTTTTCGAAATCTCATTCCGGGTATTCCG-3'.

RNA extraction and reverse transcription-quantitative PCR. Total RNA in cells was extracted using TRIzol® reagent (Invitrogen; Thermo Fisher Scientific, Inc.) according to the manufacturer's protocol. cDNA was synthesized using HiScript QRT SuperMix from the qPCR kit (Vazyme Biotech Co., Ltd.) according to the manufacturer's protocol. qPCR was performed using TransStart Top Green qPCR Super Mix (TransGen Biotech Co., Ltd.) on an ABI Step One Plus (Applied Biosystem; Thermo Fisher Scientific, Inc.). The thermocycling conditions of qPCR were as follows: 94˚C for 4 min, 30 cycles of 94˚C for 45 sec, 56˚C for 30 sec and 72˚C for 30 sec, and 72˚C for 10 min. The sequences of the primers for amplification of KRT7 were: KRT7 forward, 5'-CGAGGATATTGCCAACCGCAG-3' and reverse, 5'-CCTCAATCTCAGCCTGGAGCC-3'; and GAPDH forward, 5'-GGAGTCCACTGGCGTCTT-3' and reverse, 5'-AGTCCTTCCACGATACCAA-3' and were synthesized by GeneCopoeia, Inc. Data were quantified using the $2^{-\Delta\Delta Cq}$ method (19) and normalized to GAPDH expression in each respective sample.

Western blotting. Total cellular proteins were lysed on ice using RIPA lysis buffer [consisting of 50 mM Tris (pH 7.4), 150 mM NaCl, 1% NP-40, 0.5% sodium deoxycholate, 0.1% SDS, 100X PMSF and 100X PMSF protease inhibitor cocktail]. After the protein concentration was measured by the BCA method, 100 μg protein was loaded per lane on a 10% SDS gel, resolved using SDS-PAGE and transferred to a PVDF membrane. The PVDF membrane was blocked using TBS with 0.1% Tween-20 buffer containing 5% skimmed milk at room temperature for 2 h, incubated with primary antibodies at room temperature for 2 h, and then incubated with HRP-labeled goat anti-rabbit IgG (catalog no. S0001; Affinity Biosciences; 1:3,000) and HRP-labeled goat anti-mouse IgG (catalog no. S0002; Affinity Biosciences; 1:5,000) antibodies at room temperature for 2 h. Finally, proteins were detected using the BeyoECL Plus kit (catalog no. P0018S; Beyotime Institute of Biotechnology). The relative density of the bands was quantified using ImageJ software (version 1.52; National Institutes of Health). The following antibodies were used: Anti-KRT7 (catalog no. AF0195; Affinity Biosciences; 1:500), anti-GAPDH (catalog no. AF7021; Affinity Biosciences; 1:2,000), anti-E-cadherin (catalog no. AF0131; Affinity Biosciences; 1:1,000), anti-N-cadherin (catalog no. AF4039; Affinity Biosciences; 1:1,000), anti-vimentin (catalog no. AF7013; Affinity Biosciences; 1:1,000), anti-Snail (catalog no. AF6032; Affinity Biosciences; 1:500), anti-matrix metalloproteinase (MMP)2 (catalog no. AF0577; Affinity Biosciences; 1:1000), anti-MMP9 (catalog no. AF5228; Affinity Biosciences; 1:5,000), anti-fibronectin (FN) (catalog no. AF5335; Affinity Biosciences; 1:200), anti-integrin-β1 (catalog no. AF5379; Affinity Biosciences; 1:500), anti-FAK (catalog no. AF6397; Affinity Biosciences; 1:1,000), anti-phosphorylated (p)-FAK (catalog no. AF3398; Affinity Biosciences; 1:500), anti-Smad2/3 (catalog no. AF6367; Affinity Biosciences; 1:500), anti-phosphorylated Smad2/3 (catalog no. AF3367; Affinity Biosciences; 1:500) and anti-TGF-β1 (catalog no. AF1027; Affinity Biosciences; 1:1,000).

Transwell migration assay. Transwell experiments were performed using a CoStar Transwell chamber (8-μm pore size; BD Biosciences). HEY and OVCAR433 cells were seeded in the upper chamber at a concentration of $1x10^9$ cells/well in 300 μl serum-free medium, and the lower chamber was filled with 700 μl medium supplemented with 10% FBS to induce cell migration. The cells were incubated for 24 h at 37˚C with 5% CO_2, and the cells on the upper surface of the membrane were gently removed using a cotton swab. Cells that had migrated to the lower surface of the membrane were fixed with 4% paraformaldehyde and stained with crystal violet at room temperature. Images of the cells were obtained using a light microscope (magnification, x100).

Wound healing assay. HEY and OVCAR433 cells were seeded in 24-well plates in serum-free medium at a final concentration of $5x10^5$ cells per well. After 24 h, the cell layer was scraped with a 10-μl pipette tip to form a straight wound. After removing suspended cells with PBS, cells were grown for 48 h. Pictures of the wound area were taken under a light microscope (magnification, x100) at 0, 24 and 48 h. The difference between the wound area at different time points and 0 h was

used to calculate the cell migration rate. Each experiment was performed in triplicate.

Cell proliferation assay. HEY and OVCAR433 cell proliferation was examined using a Cell Counting Kit-8 (CCK-8) assay (catalog no. C0037; Beyotime Institute of Biotechnology) according to the manufacturer's protocol. For the assay, ~3x10^3 transfected cells were seeded in 96-well plates and cultured for 24, 48 and 72 h. Subsequently, 10 μl CCK-8 solution was added to each well and incubated for 1 h. The absorbance at 450 nm was measured at 0, 24 and 48 h using a microplate reader.

Colony formation assay. HEY and OVCAR433 cells were harvested, seeded on six-well plates (1x10^3 cells/well) and cultured for 14 days at 37˚C in a humidified incubator with 5% CO_2. The medium was changed every 3 days. After 14 days, cells were fixed with 4% paraformaldehyde and stained using crystal violet at room temperature. Clone numbers were counted by eye after photographs were obtained.

Analysis of clinical data of patients with ovarian cancer. The representative images of the immunohistochemical assay were obtained from The Human Protein Atlas (http://www.proteinatlas.org; normal patient id: 2344, tumor patient ID: 1115) (20). TCGA data for transcriptional analysis were obtained from the UALCAN database (ualcan.path.uab.edu/index.html) (21). The clinical stage and pathological grade information of patients with ovarian cancer were obtained from TCGA database (https://www.cancer.gov/tcga). The correlation analyisis between KRT7 and TGF-β1, integrin-β1 (ITGB1), MMP2 and SMAD2 expression was performed using ChIPBase version 2.0 (http://rna.sysu.edu.cn/chipbase/index.php). Differentially expressed gene analysis of KRT7 in TCGA ovarian cancer samples was performed using DECenter (Sanger Box; http://soft.sangerbox.com/). The significantly upregulated genes [log(fold-change)| ≥1.0] were analyzed by Gene Ontology (GO) enrichment using Metascape (metascape.org/) (22).

In vivo experiments. A total of 12 5-week-old female BALB/c mice (~16 g) were purchased from Charles River Laboratories, Inc., and mice were randomly divided into two groups. One group was injected with OVCAR433/shNC cells and the other group was injected with OVCAR433/shKRT7 cells. All animal experiments were performed in accordance with ethical standards of the Institutional Animal Use and Care Committee of the Affiliated Hospital of Zunyi Medical University, and ethical approval (approval no. 2019-11) was obtained from the Institutional Animal Use and Care Committee of the Affiliated Hospital of Zunyi Medical University prior to the commencement of the study. The animals were kept in a constant temperature environment of 26-28˚C and kept in light for 10 h a day. All drinking water and food were sterilized and provided *ad libitum*. OVCAR433/shNC and OVCAR433/shKRT7 cells (2x10^6 cells) were subcutaneously injected into nude mice (n=6 per group). Tumor volumes were monitored every 3 days and animal health was continuously monitored throughout the study. The tumor volume was calculated as follows: Volume = (length x $width^2$)/2. A total of 1 month after injection, all animals were euthanized through intravenous injection of sodium pentobarbital at a final concentration of 100 mg/kg. The mice were checked for >5 min and death was confirmed by observing lack of respiration and cardiac output. Subsequently, the solid tumors were harvested from the mice by surgery. All tissues were fixed in 4% formalin and embedded in paraffin for immunohistochemical staining.

Embedded tumor tissues were cut into sections (4-μm thickness) and treated with 3% hydrogen peroxide for 10 min to inhibit endogenous peroxidase activity. Subsequently, 5% bovine serum albumin (Shanghai Shenggong Biology Engineering Technology Service, Ltd.) was used to block non-specific binding at 37˚C for 30 min. Tissue sections were treated with primary antibodies against E-cadherin (catalog no. AF0131; Affinity Biosciences; 1:200) and vimentin (catalog no. AF7013; Affinity Biosciences; 1:200) and incubated overnight in a humidified chamber at 4˚C. Sections were visualized using 3,3-diaminobenzidine at room temperature for 5 min and counterstained with hematoxylin for 1 min at room temperature. Then pictures were examined under a light microscope (magnification, x100). The expression levels of E-cadherin and Vimentin protein in the tumor were scored based on the staining intensity and the percentage of positively stained cells. Six fields were randomly selected for each slice. The scoring system used was as follows: Staining intensity x number of cells with positive scores. Staining intensity: 0, no positive cells; 1, yellow staining; 2, light brown staining; and 3, dark brown staining. Percentage of cells with positive scores: 1, <25%; 2, 25-50%; 3, 51-75%; 4, >75%).

Statistical analysis. All statistical analyses were performed using SPSS version 19.0 (IBM Corp.). Significant differences between two groups were compared using an unpaired Student's t-test. Comparisons of KRT7 expression levels between ovarian cancer tissues and adjacent normal tissues were analyzed using a paired Student's t-test. Comparisons among three or more groups were conducted using ANOVA with post hoc Student-Newman-Keuls test. The correlation between KRT7 expression and clinicopathological factors was estimated using Pearson's correlation analysis. The relationship between the survival rate and KRT7 expression was analyzed using the Kaplan-Meier method. $P<0.05$ was considered to indicate a statistically significant difference.

Results

KRT7 expression is upregulated in ovarian cancer tissues. To investigate the clinical significance of KRT7 in ovarian cancer, the expression levels of KRT7 in ovarian cancer tissues and adjacent normal tissues was determined using the data obtained from the Human Protein Atlas. The expression of KRT7 protein was analyzed by immunohistochemical staining in tumor tissues and corresponding normal (non-tumor) tissues. The representative images and final scoring results are shown in Fig. 1A. There was a significant increase in KRT7 staining in cancer tissues compared with adjacent normal tissues. Analysis of data obtained from TCGA demonstrated that KRT7 mRNA expression was higher in tumor tissues compared with normal tissues (Fig. 1B). By analyzing TCGA data, KRT7 expression levels in grade 3 samples were found

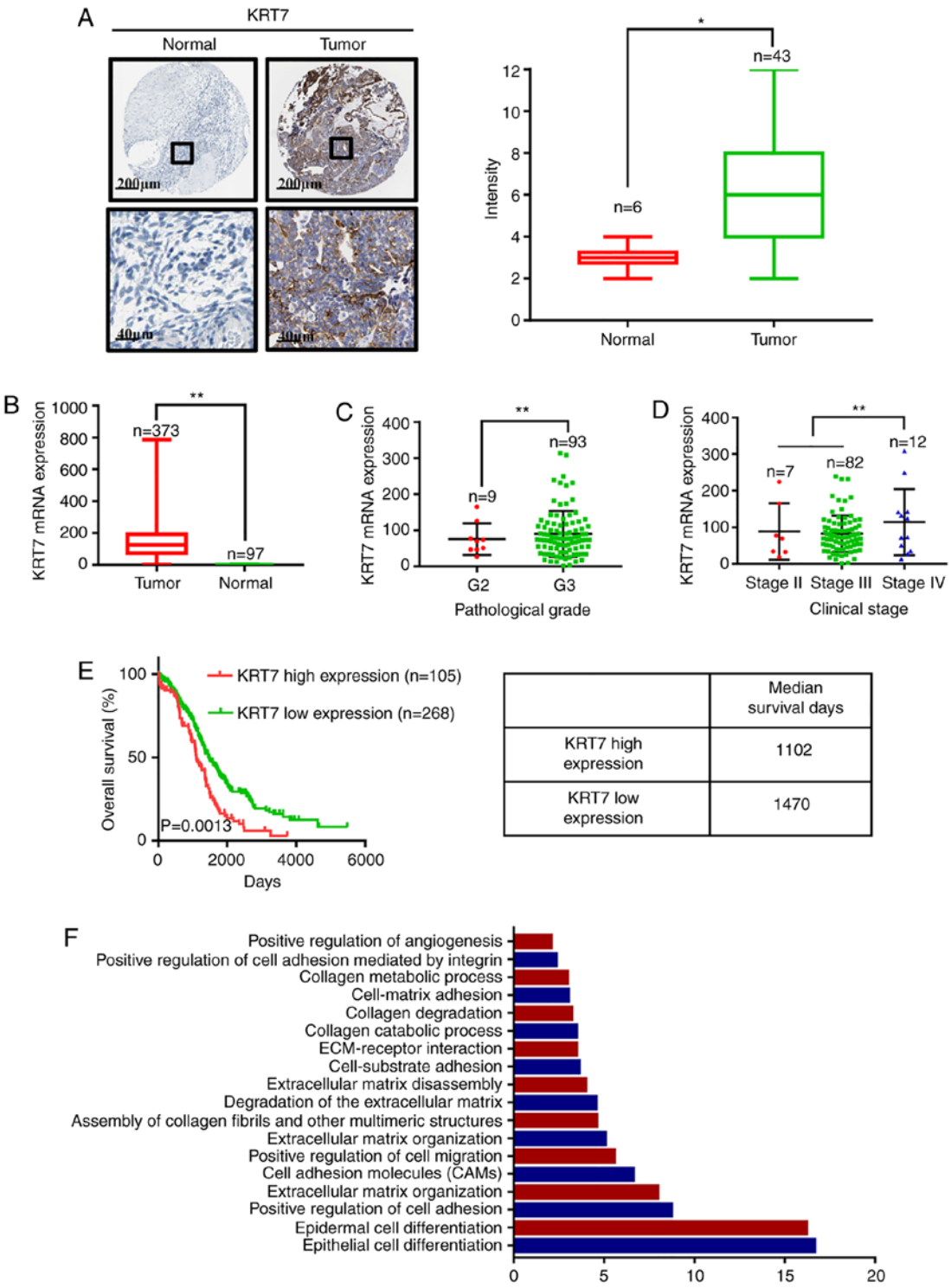

Figure 1. KRT7 expression is indicative of a poor prognosis in patients with ovarian cancer. (A) Representative images of KRT7 staining in normal and ovarian tumor tissues, and immunohistochemical score of KRT7 in normal and ovarian tumor tissues. (B) mRNA expression levels of KRT7 in normal and ovarian tumor tissues. Associations between the (C) pathological grades and (D) clinical stages of ovarian cancer with KRT7 expression. (E) Effect of mRNA expression levels of KRT7 on the median survival time of patients with ovarian cancer. (F) Gene Ontology analysis of the differentially expressed genes between the high- and low-expression KRT7 groups in patients with ovarian cancer. Data were obtained from the Human Protein Atlas and The Cancer Genome Atlas database. *P<0.05, **P<0.01. KRT7, keratin 7; ECM, extracellular matrix.

to be higher than that in grade 2 samples (Fig. 1C). In addition, KRT7 expression was observed to be the highest in patients with clinical stage IV ovarian cancer (Fig. 1D).

KRT7 expression levels are associated with the survival of patients with ovarian cancer. To further elucidate the role of KRT7 in the survival of patients with ovarian cancer, data obtained from TCGA were used to determine the relationship between KRT7 mRNA expression and survival in patients with ovarian cancer. Kaplan-Meier analysis showed that the median survival of patients with high and low KRT7 expression levels was 1,102 and 1,470 days, respectively, indicating a poorer

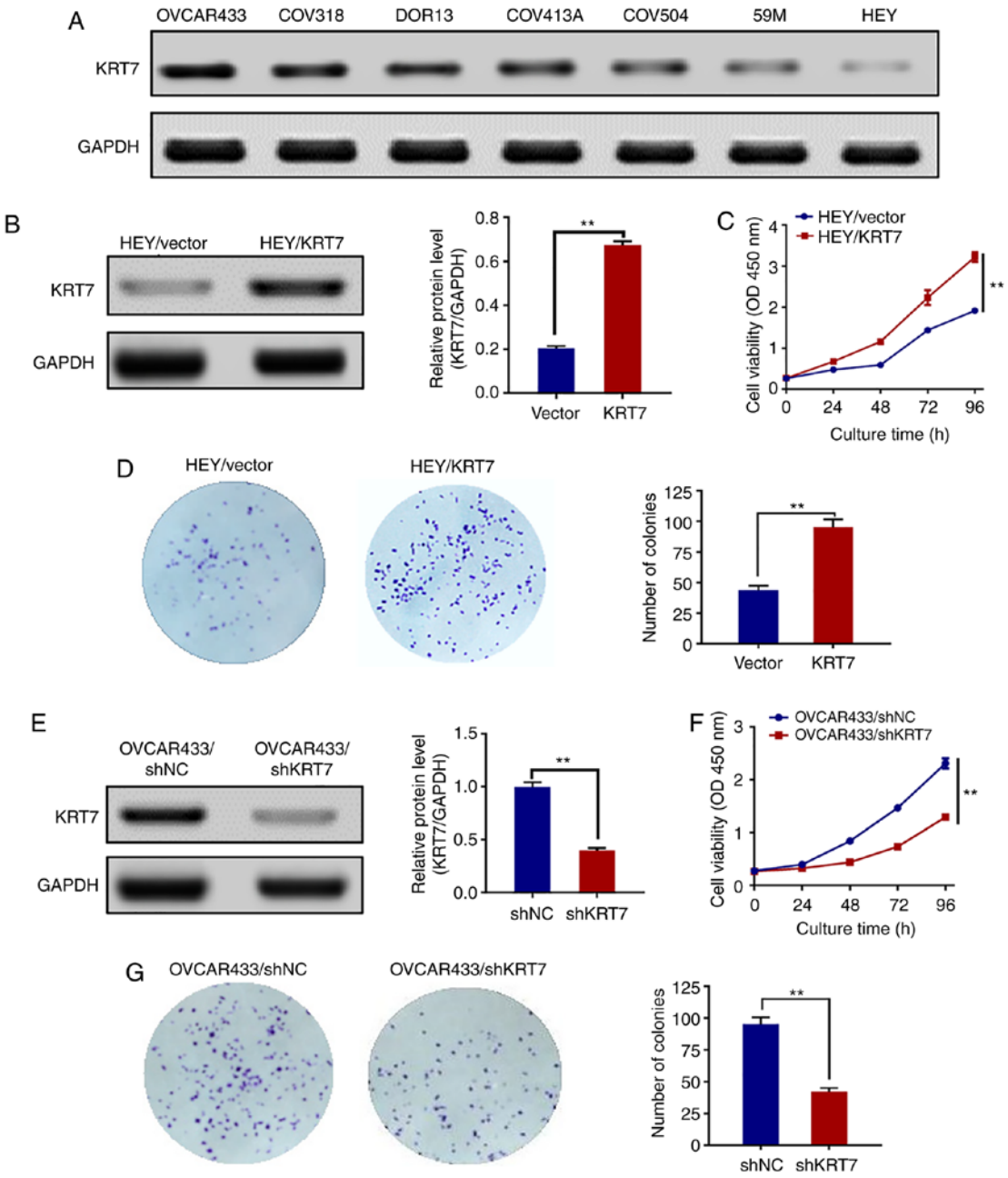

Figure 2. Effect of KRT7 on HEY and OVCAR433 cell proliferation and colony formation. (A) Protein expression levels of KRT7 in ovarian cell lines were assessed using western blotting. (B) Overexpression of KRT7 in HEY cells was confirmed by western blotting. (C) Overexpression of KRT7 significantly increased the proliferative capacity of HEY cells. (D) Overexpression of KRT7 in HEY cells significantly increased colony formation. (E) Knockdown of KRT7 in OVCAR433 cells was confirmed by western blotting. Knockdown of KRT7 in OVCAR433 cells significantly reduced (F) cell proliferation and (G) colony formation. All experiments were performed at least three times. Results are presented as the mean ± standard deviation. **P<0.01. KRT7, keratin 7; sh, short hairpin RNA; NC, negative control; OD, optical density.

prognosis in patients with high KRT7 expression (Fig. 1E). After stratifying ovarian cancer patient data from TCGA based on KRT7 expression levels, the differentially expressed genes between the high- and low-expression groups were determined. GO enrichment analysis results showed that KRT7 is associated with 'positive regulation of cell migration' and 'positive regulation of angiogenesis' (Fig. 1F). Therefore, upregulated KRT7 expression may promote the malignant progression of ovarian cancer in patients.

KRT7 expression levels in human ovarian cancer cell lines. To examine the expression levels of KRT7 in human ovarian cancer cell lines, seven cell lines (HEY, 59M, COV504, COV413A, DOR13, COV318 and OVCAR433) were analyzed by western blotting. KRT7 protein was expressed in all seven human ovarian cancer cell lines. The expression of the KRT7 protein was the highest and lowest in the OVCAR433 and HEY cell lines, respectively (Fig. 2A). Therefore, OVCAR433 and HEY cells were used for the subsequent experiments.

KRT7 overexpression affects ovarian cancer cell proliferation. To investigate whether KRT7 affected ovarian cancer cell proliferation, HEY cells were transfected with pcDNA3.1/KRT7 to enhance KRT7 expression, and HEY

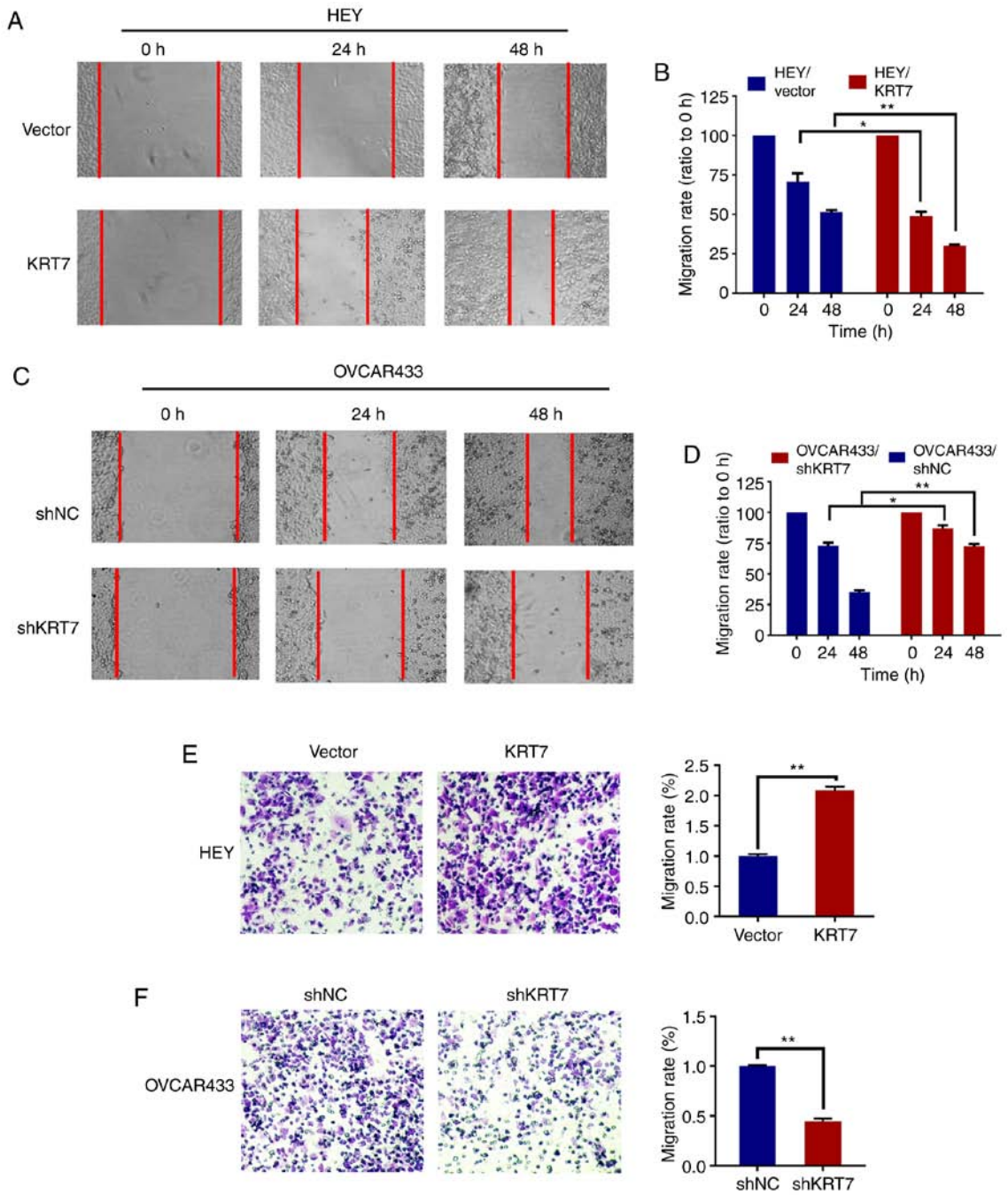

Figure 3. KRT7 overexpression enhances migration of ovarian cancer cells. (A and B) Overexpression of KRT7 increased the wound healing capacity of HEY cells. (C and D) Knockdown of KRT7 reduced the wound healing capacity of OVCAR433 cells. (E) Overexpression of KRT7 promoted the migration capacity of HEY cells. (F) Knockdown of KRT7 reduced the migration capacity of OVCAR433 cells. All experiments were performed at least three times. Results are presented as the mean ± standard deviation. *P<0.05, **P<0.01. KRT7, keratin 7; sh, short hairpin RNA; NC, negative control.

cells transfected with pcDNA3.0 blank vector were used as a control. KRT7 overexpression in HEY cells was confirmed by western blotting (Fig. 2B). Thereafter, the proliferation of pcDNA3.0-KRT7 and pcDNA3.0 (blank vector) HEY cells was assayed using the CCK-8 assay. KRT7 overexpression significantly increased HEY cell proliferation (Fig. 2C) and resulted in increased colony formation compared with the control cells (Fig. 2D). KRT7 expression in OVCAR433 cells was then knocked down using shRNA (Fig. 2E). The proliferation and colony formation abilities of OVCAR433 cells transfected with si-KRT7 were decreased compared with the control group (Fig. 2F and G). Results of colony formation suggest that KRT7 can promote the proliferation of ovarian cancer cells and may affect the stemness of the cells.

KRT7 affects the migration of ovarian cancer cells. To evaluate the effect of KRT7 on ovarian cell migration, a wound healing assay with HEY and OVCAR433 cells was used. Compared with the vector group, the cell migration rate was significantly increased following KRT7 overexpression in HEY cells (Fig. 3A and B). In KRT7 -knockdown OVCAR433 cells, the migration rate decreased significantly (Fig. 3C and D). The effect of KRT7 on ovarian cell migration was verified using a Transwell assay. The results demonstrated that KRT7

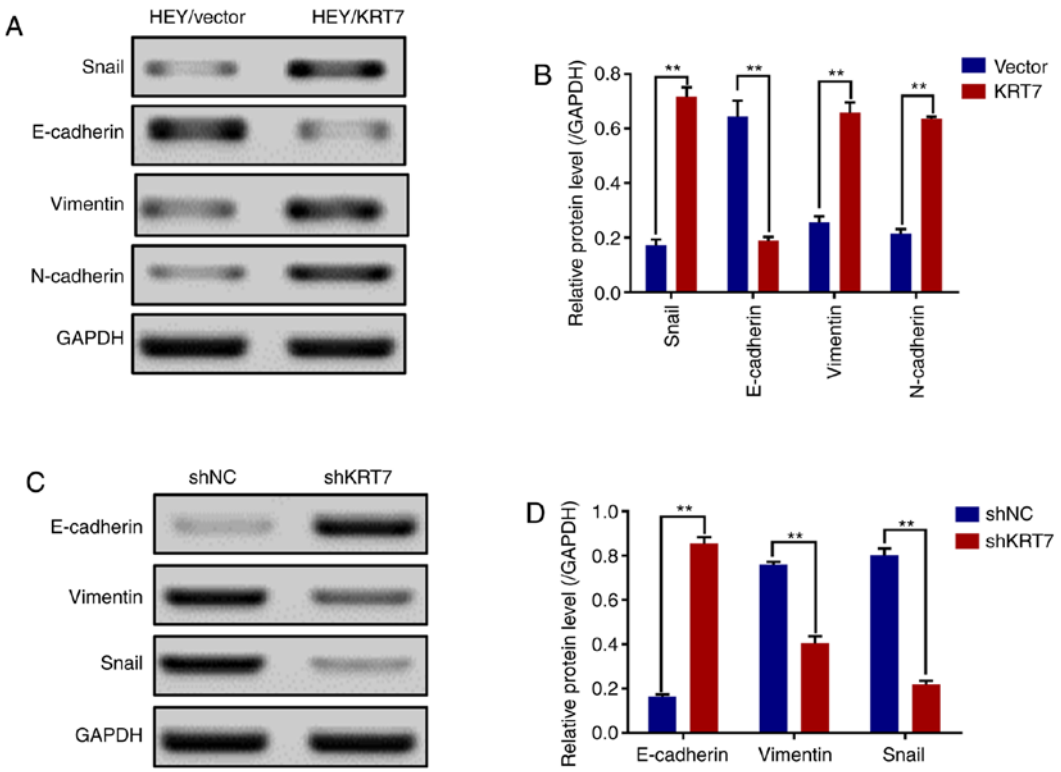

Figure 4. KRT7 expression affects epithelial-mesenchymal transition in HEY and OVCAR433 cells. (A and B) Overexpression of KRT7 increased Snail, vimentin and N-cadherin expression, and decreased E-cadherin expression in HEY cells as detected by western blotting. (C and D) Knockdown of KRT7 resulted in increased E-cadherin expression and reduced vimentin and Snail expression in OVCAR433 cells as detected by western blotting. All experiments were performed at least three times. Results are presented as the mean ± standard deviation. **P<0.01. KRT7, keratin 7; sh, short hairpin RNA; NC, negative control.

overexpression significantly increased the number of migrating HEY cells compared with the vector group (Fig. 3E). By contrast, KRT7 knockdown significantly reduced the number of invading OVCAR433 cells (Fig. 3F).

KRT7 overexpression induces EMT of ovarian cancer cells. Before migration and invasion of epithelial cells can occur, there are genotypic and morphological changes which occur; collectively referred to as EMT. Snail, vimentin, N-cadherin and E-cadherin are EMT markers (23). The results demonstrated that the expression levels of Snail, vimentin and N-cadherin were significantly increased, and that of E-cadherin was significantly decreased in HEY cell lines overexpressing KRT7 (Fig. 4A and B). By contrast, KRT7 knockdown in OVCAR433 cells significantly increased E-cadherin expression and significantly decreased vimentin and Snail expression (Fig. 4C and D). In summary, these data suggest that KRT7 regulates EMT, resulting in the increased migratory capacity of ovarian cancer cells *in vitro*.

KRT7 overexpression increases cell-matrix adhesion through integrin-β1-FAK signaling. Increasing cell-matrix adhesion is an important step in tumor cell metastasis (24). The role of KRT7 in regulating cell-matrix adhesion in ovarian cancer cells was investigated by detecting the expression of FN, integrin-β1, FAK and other genes involved in proliferation and migration. Western blotting revealed that the expression levels of PCNA, FN, MMP9, integrin-β1 and p-FAK/FAK (Tyr397) were increased, but TIMP-1 was decreased in HEY cells overexpressing KRT7 (Fig. 5A-D). By contrast, KRT7 knockdown decreased MMP2 and MMP9 expression in OVCAR433 cells (Fig. 5E). Thus, the adhesion-promoting effect of KRT7 overexpression was likely mediated through integrin-β1-FAK signaling.

KRT7-induced EMT and cell migration are mediated by TGF-β signaling. Several pathways regulate cancer cell EMT and migration. One of the key mechanisms by which TGF-β promotes cell migration, invasion and metastasis is through induction of EMT (25). Thus, whether KRT7-induced EMT was mediated by the TGF-β signaling pathway was determined. TGF-β1, Smad2/3 and p-Smad2/3, which are important downstream regulators of the TGF-β signaling pathway, were detected in the present study. The results showed that the levels of p-Smad2/3/Smad2/3 in KRT7-overexpressing HEY cells was significantly increased (Fig. 5F). The levels of p-Smad2/3/Smad2/3 in KRT7 knockdown OVCAR433 cells was decreased (Fig. 5G). These data suggest that KRT7 can partially promote cellular EMT and migration by activating the TGF-β/Smad2/3 pathway. To verify the aforementioned molecular mechanism, ChIPBase was used to analyze the correlation of KRT7 protein expression with TGF-β1, ITGB1, MMP2 and SMAD2 protein expression in patients with ovarian cancer. The results demonstrated that KRT7 expression levels were positively correlated with the expression of TGF-β1, ITG-β1, MMP2 and SMAD2 (Fig. 6A-D), verifying the role of KRT7 in EMT and cell migration through the TGF-β pathway.

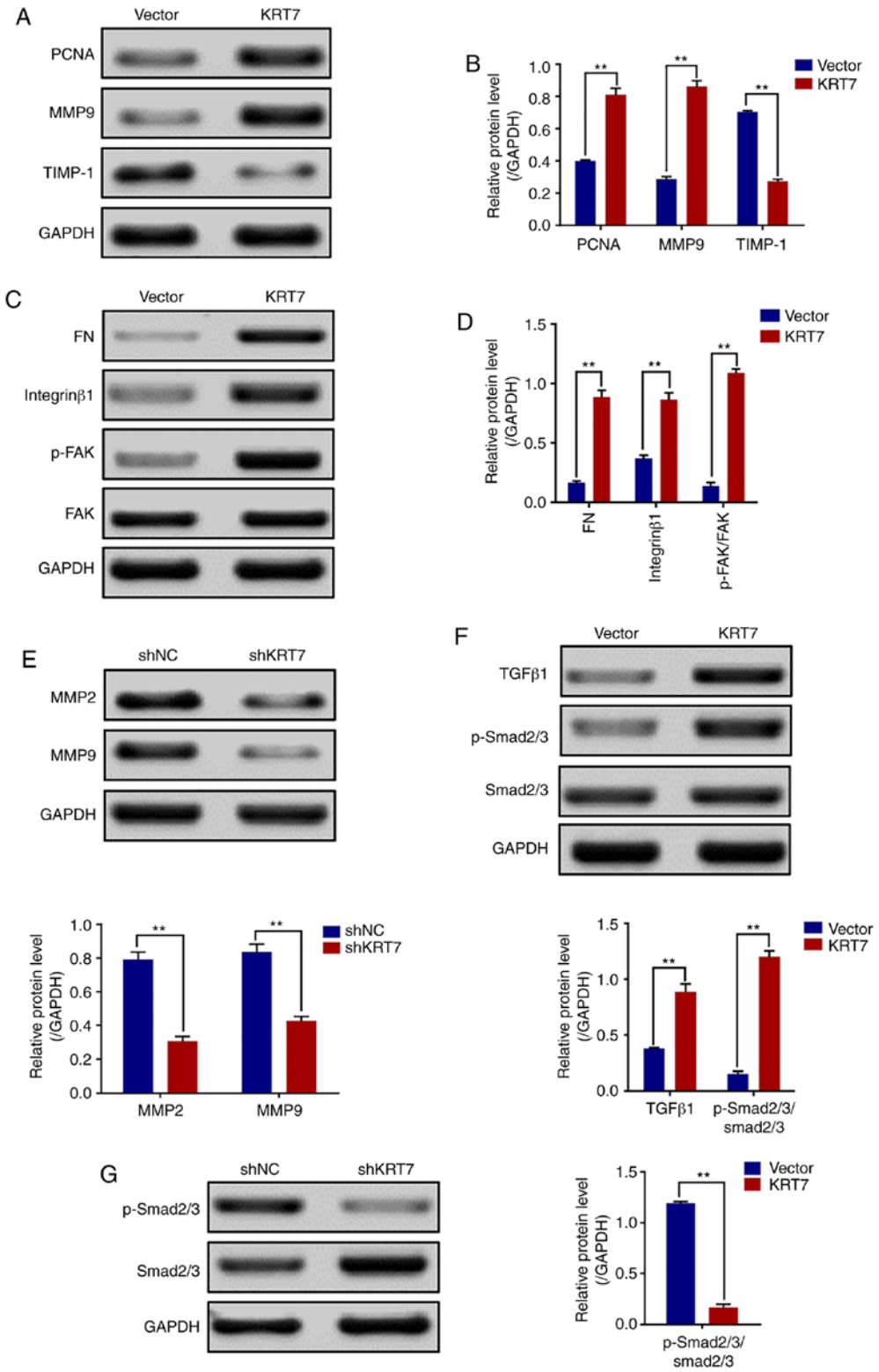

Figure 5. KRT7 expression affects the integrin-β1-FAK signaling and TGF-β signaling pathways. (A and B) Expression of proliferation- and migration-associated genes (PCNA, MMP9 and TIMP-1) were evaluated using western blotting in HEY cells. (C and D) Western blotting of proteins involved in integrin-β1-FAK signaling pathway in the KRT7-overexpressing HEY cells. (E) Expression of MMPs after knockdown of KRT7 in OVCAR433 cells. (F and G) Expression of the TGF-β signaling pathway-related proteins was evaluated by western blotting in KRT7-overexpressing HEY cells and KRT7-knockdown OVCAR433 cells. All experiments were performed at least three times. Results are presented as the mean ± standard deviation. **P<0.01. FAK, focal adhesion kinase; PCNA, proliferating cell nuclear antigen; FN, fibronectin; TIMP-1, TIMP metallopeptidase inhibitor 1; p-, phosphorylated; MMP, matrix metalloproteinase; KRT7, keratin 7; sh, short hairpin RNA; NC, negative control.

TGF-β1 counteracts the inhibition of KRT7 knockdown on OVCAR433 cells. To verify whether the function of KRT7 in ovarian cancer cells was dependent on the TGF-β1 pathway, TGF-β1 was overexpressed in the KRT7-knockdown OVCAR433 cells. Western blotting was used to detect TGF-β1 and p-Smad2/3. The results demonstrated that TGF-β1 could increase the ratio

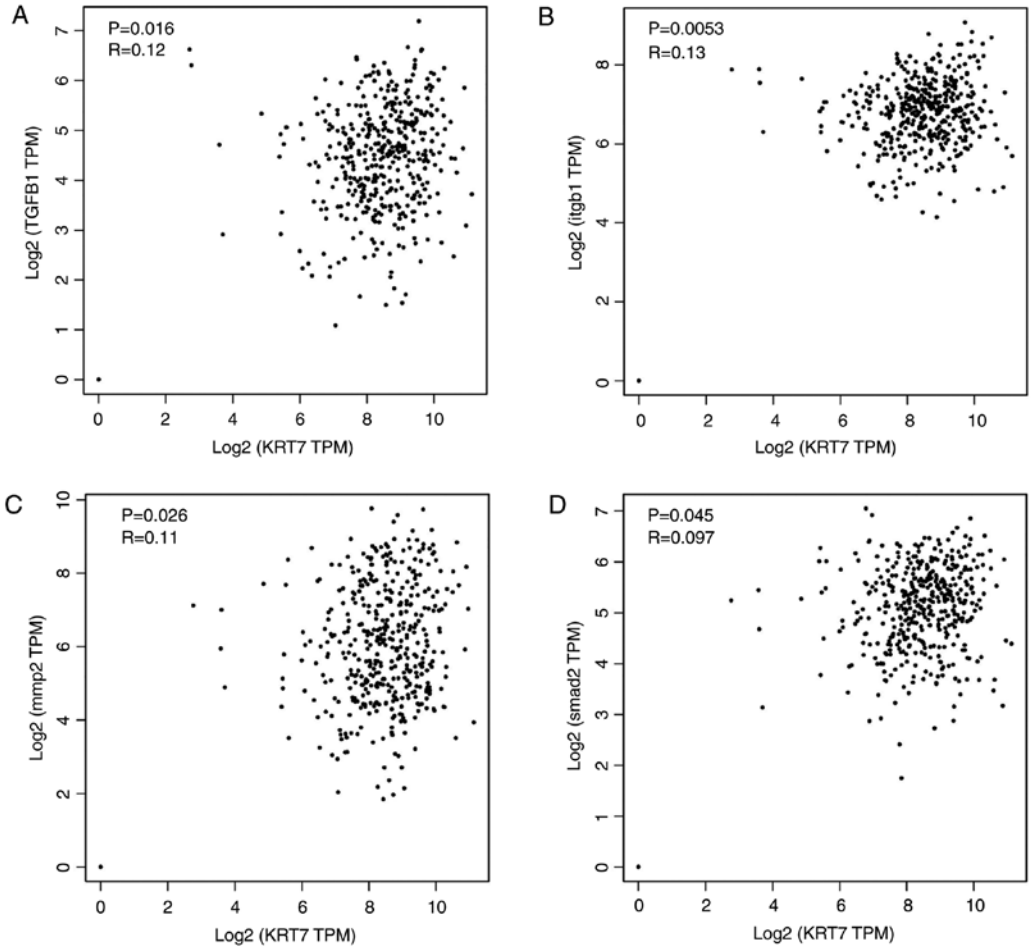

Figure 6. Correlation between KRT7 expression levels with TGF-β1, ITGB1, MMP2 and SMAD2. Correlation of KRT7 protein expression in patients with ovarian cancer with (A) TGF-β1, (B) ITGB1, (C) MMP2 and (D) SMAD2 protein expression levels. The expression information of ovarian cancer samples was obtained from The Cancer Genome Atlas for correlation analysis. KRT7, keratin 7; MMP, matrix metalloproteinase; ITGB1, integrin-β-1; TPM, transcripts per million.

of p-Smad2/3/Smad2/3. Following confirmation of overexpression (Fig. 7A), the results of the Transwell and would healing experiments showed that the overexpression of TGF-β1 restored the inhibitory effects of KRT7 knockdown (Fig. 7B and C). In addition, colony formation assays also showed similar results (Fig. 7D). These results suggest that the role of KRT7 in ovarian cancer cells is partially dependent on the TGF-β1 pathway.

KRT7 knockdown inhibits tumor growth in vivo. Tumor-bearing mice were established using KRT7-knockdown OVCAR433 stable cells. Tumor growth in the KRT7 knockdown group was significantly inhibited compared with the control group (Fig. 8A-C). Immunohistochemical staining of E-cadherin and vimentin in the tumors showed significantly higher expression of E-cadherin and significantly lower expression of vimentin in the KRT7 knockdown group compared with the control group (Fig. 8D and E). These data suggest that KRT7 knockdown may inhibit tumor growth *in vivo*.

Discussion

Although KRT7 has been reported to be overexpressed in several types of malignant tumors, including gastric cancer and ovarian cancer, and is associated cell proliferation, EMT and stemness (26,27). The abnormal expression and possible roles of KRT7 in ovarian cancer have not been reported previously, to the best of our knowledge. In the present study, KRT7 expression in ovarian cancer cells was significantly higher compared with the normal tissues. The upregulated expression of KRT7 resulted in the migration of cancer cells and in the alteration in the expression levels of a series of EMT-related genes, which decreased the survival time of patients. The present study also demonstrated that the abnormal expression of KRT7 regulated changes in extracellular matrix (ECM) and collagen-associated genes, resulting in cancer cell migration.

The ECM provides biophysical and biochemical signals that regulate cell proliferation, differentiation, migration and invasion. It is a dynamic environment that constantly influences cell response (28). ECM and its modifications are key factors involved in determining metastatic tumor formation (29). In several types of solid cancer, the increased expression of matrix proteins is associated with increased mortality (30). In addition, changes in matrix hardness and fibrosis, and excessive deposition of fibrous ECM components (primarily collagen) are associated with tumor progression (31). Changes in the structure and hardness of ECM result in changes in cellular mechanical transduction, and the associated molecular pathways are considered potential targets for treatment of cancer (32). The key role of ECM in tumor migration and metastasis is the expression of ECM receptor (integrin) on the surface of tumor cells and the

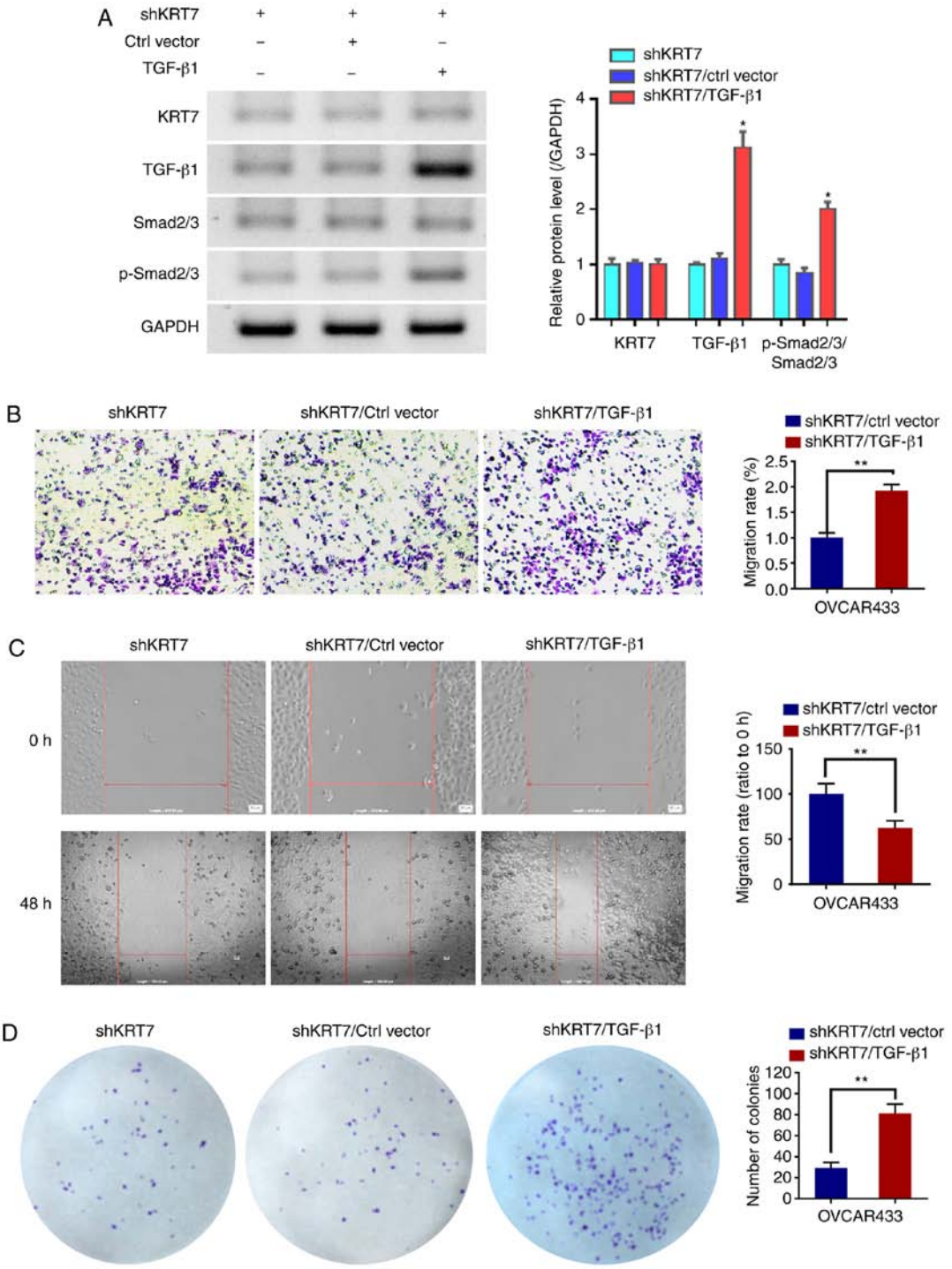

Figure 7. TGF-β1 promotes OVCAR433 cell progression. A TGF-β1 overexpression plasmid was transfected into KRT7 knockdown OVCAR433 cells. (A) Protein expression levels of KRT7, TGF-β1, Smad2/3 and p-Smad2/3. *P<0.05 vs. shKRT7/ctrl vector. (B) Transwell assays were used to detect cell migration. Magnification, x100. (C) Wound healing assays were performed to assess cell migration. Magnification, x100. (D) Colony formation assays were performed to detect cell proliferation. **P<0.01. p-, phosphorylated; KRT7, keratin 7; sh, short hairpin RNA; Ctrl, control.

ability of tumor cells to degrade the ECM through MMPs (33). Therefore, the increase in integrin-β1 and MMP9 expression is associated with cancer cell migration. MMP-9 is the primary target of colonial migration, which is associated with a high invasive capacity of cancer cells (34). FAK is a downstream target of integrin and an important signaling molecule regulating the cell response (35). In the present study, the expression levels of FAK and integrin-β1 were upregulated when KRT7 was overexpressed, suggesting that KRT7 can regulate the degradation of the cancer cell ECM, thereby enhancing the invasive capacity of cells.

TGF-β signal transduction is closely associated with cancer and serves a dual role in tumorigenesis (36). Generally, TGF-β inhibits cell proliferation and stimulates normal cell differentiation; thus, it can be used as a tumor suppressor (37). However, in advanced stage cancer, TGF-β promotes tumor progression and metastasis, thus acting as a carcinogen (37). TGF-β-induced EMT supports tumor invasion and transmission by releasing

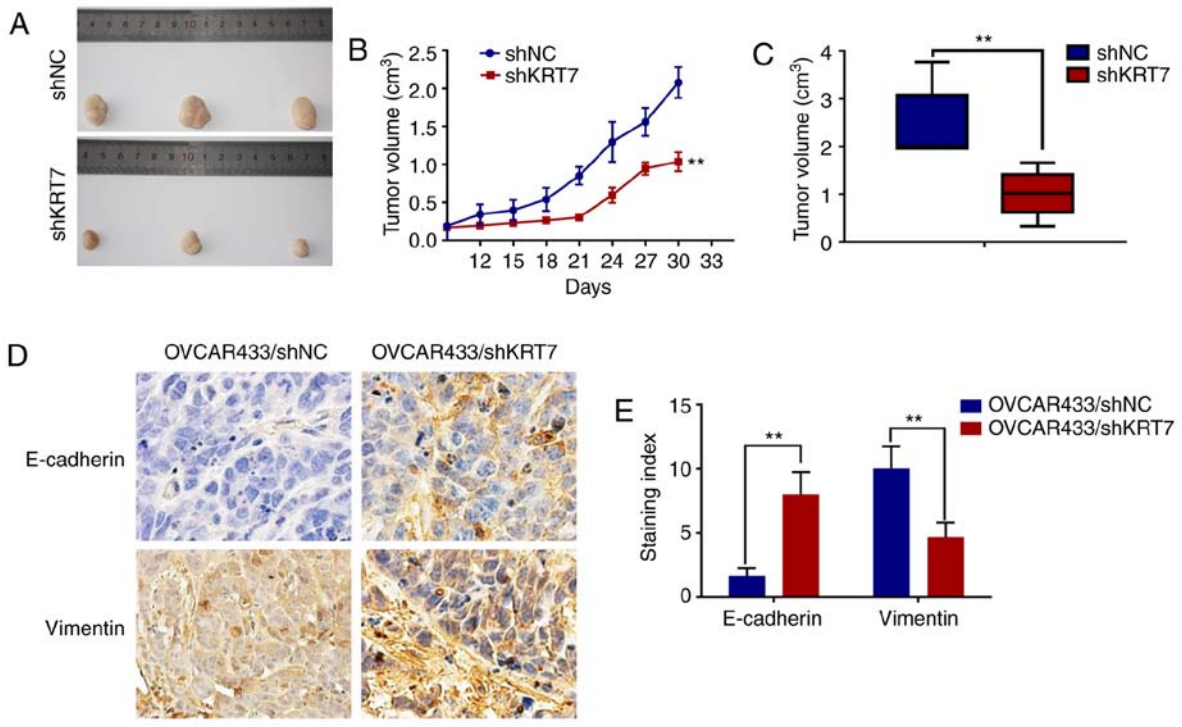

Figure 8. KRT7 knockdown inhibits tumor growth *in vivo*. (A) Tumor growth was reduced in the KRT7 knockdown group. (B and C) Changes in the tumor volume in each group. (D and E) Immunohistochemical staining for E-cadherin and vimentin protein expression in the tumor samples from the xenografts. Magnification, x100. **P<0.01. KRT7, keratin 7; sh, short hairpin RNA; NC, negative control.

tumor cells into the surrounding environment and promoting their movement (38). In several types of cancer, TGF-β-induced EMT transcription regulates E-cadherin, Snail, N-cadherin and vimentin. It also induces Sox4 expression and promotes mesenchymal transition, facilitating tumor progression and cancer cell invasion (39-41). In the present study, KRT7 was shown to be involved in EMT through TGF-β signaling, which in turn resulted in increased ovarian cancer cell migration. E-cadherin protein expression was decreased in KRT7-overexpressing ovarian cancer cells, whereas expression of MMP9, FN and TGF-β signaling (TGF-β1 and p-Smad2/3) pathway-associated proteins was increased. Therefore, KRT7 enhanced EMT through the TGF-β/Smad2/3 signaling pathway and promoted the progression of cancer.

In conclusion, the present study demonstrated that upregulated expression of KRT7 was associated with ovarian cancer cell migration and EMT pathways, thereby promoting ovarian cancer progression, such as tumor invasion depth, and leading to decreased survival. Therefore, KRT7 may serve as a potential target for treatment of ovarian cancer.

Acknowledgements

The results shown here are in whole or part based upon data generated by the TCGA Research Network: https://www.cancer.gov/tcga.

Funding

This study was supported by the Science and Technology Foundation of Guizhou Provincial Science and Technology Department (grant no. JLKZ201120).

Availability of data and materials

The datasets used and/or analyzed during the present study are available from the corresponding author on reasonable request.

Authors' contributions

BY conceived and designed the study. QA performed all the experiments. TL, MYW, YJY, ZDZ and ZJL analyzed the data. All authors read and approved the final manuscript.

Ethics approval and consent to participate

All animal experiments were performed in accordance with ethical standards of the Institutional Animal Use and Care Committee of the Affiliated Hospital of Zunyi Medical University, and ethical approval (approval no. 2019-11) was obtained prior to the commencement of the study.

Patient consent for publication

Not applicable.

Competing interests

The authors declare that they have no competing interests.

References

1. Coukos G, Tanyi J and Kandalaft LE: Opportunities in immunotherapy of ovarian cancer. Ann Oncol 27 (Suppl 1): i11-i15, 2016.

2. Smith RA, Andrews KS, Brooks D, Fedewa SA, Manassaram-Baptiste D, Saslow D, Brawley OW and Wender RC: Cancer screening in the United States, 2017: A review of current American Cancer Society guidelines and current issues in cancer screening. CA Cancer J Clin 67: 100-121, 2017.
3. US Preventive Services Task Force; Grossman DC, Curry SJ, Owens DK, Barry MJ, Davidson KW, Doubeni CA, Epling JW Jr, Kemper AR, Krist AH, *et al*: Screening for ovarian cancer: US preventive services task force recommendation statement. JAMA 319: 588-594, 2018.
4. Siegel RL, Miller KD and Jemal A: Cancer statistics. CA Cancer J Clin 68: 7-30, 2018.
5. Corrado G, Salutari V, Palluzzi E, Distefano MG, Scambia G and Ferrandina G: Optimizing treatment in recurrent epithelial ovarian cancer. Expert Rev Anticancer Ther 17: 1147-1158, 2017.
6. Bristow RE and Chi DS: Platinum-based neoadjuvant chemotherapy and interval surgical cytoreduction for advanced ovarian cancer: A meta-analysis. Gynecol Oncol 103: 1070-1076, 2006.
7. Derynck R and Weinberg RA: EMT and cancer: More than meets the eye. Dev Cell 49: 313-316, 2019.
8. Feng W, Dean DC, Hornicek FJ, Shi H and Duan Z: Exosomes promote pre-metastatic niche formation in ovarian cancer. Mol Cancer 18: 124, 2019.
9. Javan Maasomi Z, Pilehvar Soltanahmadi Y, Dadashpour M, Alipour S, Abolhasani S and Zarghami N: Synergistic anticancer effects of silibinin and chrysin in T47D breast cancer cells. Asian Pac J Cancer Prev 18: 1283-1287, 2017.
10. Sandilands A, Smith FJ, Lunny DP, Campbell LE, Davidson KM, MacCallum SF, Corden LD, Christie L, Fleming S, Lane EB and McLean WH: Generation and characterisation of keratin 7 (K7) knockout mice. PLoS One 8: e64404, 2013.
11. Woods RSR, Keegan H, White C, Tewari P, Toner M, Kennedy S, O'Regan EM, Martin CM, Timon CVI and O'Leary JJ: Cytokeratin 7 in oropharyngeal squamous cell carcinoma: A junctional biomarker for human papillomavirus-related tumors. Cancer Epidemiol Biomarkers Prev 26: 702-710, 2017.
12. Hosoya A, Kwak S, Kim EJ, Lunny DP, Lane EB, Cho SW and Jung HS: Immunohistochemical localization of cytokeratins in the junctional region of ectoderm and endoderm. Anat Rec (Hoboken) 293: 1864-1872, 2010.
13. Karantza V: Keratins in health and cancer: More than mere epithelial cell markers. Oncogene 30: 127-138, 2011.
14. Oue N, Noguchi T, Anami K, Kitano S, Sakamoto N, Sentani K, Uraoka N, Aoyagi K, Yoshida T, Sasaki H and Yasui W: Cytokeratin 7 is a predictive marker for survival in patients with esophageal squamous cell carcinoma. Ann Surg Oncol 19: 1902-1910, 2012.
15. Harbaum L, Pollheimer MJ, Kornprat P, Lindtner RA, Schlemmer A, Rehak P and Langner C: Keratin 7 expression in colorectal cancer-freak of nature or significant finding? Histopathology 59: 225-234, 2011.
16. Lambaudie E, Chereau E, Pouget N, Thomassin J, Minsat M, Charafe-Jauffret E, Jacquemier J and Houvenaeghel G: Cytokeratin 7 as a predictive factor for response to concommitant radiochemotherapy for locally advanced cervical cancer: A preliminary study. Anticancer Res 34: 177-181, 2014.
17. Kuroda H, Imai Y, Yamagishi H, Ueda Y, Kuroso K, Oishi Y, Ohashi H, Yamashita A, Yashiro Y and Fukushima H: Aberrant keratin 7 and 20 expression in triple-negative carcinoma of the breast. Ann Diagn Pathol 20: 36-39, 2016.
18. Wang P, Magdolen V, Seidl C, Dorn J, Drecoll E, Kotzsch M, Yang F, Schmitt M, Schilling O, Rockstroh A, *et al*: Kallikrein-related peptidases 4, 5, 6 and 7 regulate tumour-associated factors in serous ovarian cancer. Br J Cancer 119: 1-9, 2018.
19. Livak KJ and Schmittgen TD: Analysis of relative gene expression data using real-time quantitative PCR and the 2(-Delta Delta C(T)) method. Methods 25: 402-408, 2001.
20. Uhlén M, Fagerberg L, Hallström BM, Lindskog C, Oksvold P, Mardinoglu A, Sivertsson Å, Kampf C, Sjöstedt E, Asplund A, *et al*: Proteomics. Tissue-based map of the human proteome. Science 347: 1260419, 2015.
21. Chandrashekar DS, Bashel B, Balasubramanya SA, Creighton CJ, Ponce-Rodriguez I, Chakravarthi BV and Varambally S: UALCAN: A portal for facilitating tumor subgroup gene expression and survival analyses. Neoplasia 19: 649-658, 2017.
22. Zhou Y, Zhou B, Pache L, Chang M, Khodabakhshi AH, Tanaseichuk O, Benner C and Chanda SK: Metascape provides a biologist-oriented resource for the analysis of systems-level datasets. Nat Commun 10: 1523, 2019.
23. Pastushenko I and Blanpain C: EMT transition states during tumor progression and metastasis. Trends Cell Biol 29: 212-226, 2019.
24. Kai F, Drain AP and Weaver VM: The extracellular matrix modulates the metastatic journey. Dev Cell 49: 332-346, 2019.
25. Cantelli G, Orgaz JL, Rodriguez-Hernandez I, Karagiannis P, Maiques O, Matias-Guiu X, Nestle FO, Marti RM, Karagiannis SN and Sanz-Moreno V: TGF-β-induced transcription sustains amoeboid melanoma migration and dissemination. Curr Biol 25: 2899-2914, 2015.
26. Huang B, Song JH, Cheng Y, Abraham JM, Ibrahim S, Sun Z, Ke X and Meltzer SJ: Long non-coding antisense RNA KRT7-AS-as is activated in gastric cancers and supports cancer cell progression by increasing krt7 expression. Oncogene 35: 4927-4936, 2016.
27. Tajima Y, Ito K, Umino A, Wilkinson AC, Nakauchi H and Yamazaki S: Continuous cell supply from Krt7-expressing hematopoietic stem cells during native hematopoiesis revealed by targeted in vivo gene transfer method. Sci Rep 7: 40684, 2017.
28. Lu P, Weaver VM and Werb Z: The extracellular matrix: A dynamic niche in cancer progression. J Cell Biol 196: 395-406, 2012.
29. Filipe EC, Chitty JL and Cox TR: Charting the unexplored extracellular matrix in cancer. Int J Exp Pathol 99: 58-76, 2018.
30. Alexander J and Cukierman E: Stromal dynamic reciprocity in cancer: Intricacies of fibroblastic-ECM interactions. Curr Opin Cell Biol 42: 80-93, 2016.
31. Byron A, Humphries JD and Humphries MJ: Defining the extracellular matrix using proteomics. Int J Exp Pathol 94: 75-92, 2013.
32. Pickup MW, Mouw JK and Weaver VM: The extracellular matrix modulates the hallmarks of cancer. EMBO Rep 15: 1243-1253, 2014.
33. Piwko-Czuchra A, Koegel H, Meyer H, Bauer M, Werner S, Brakebusch C and Fässler R: Beta1 integrin-mediated adhesion signalling is essential for epidermal progenitor cell expansion. PLoS One 4: e5488, 2009.
34. Khan Z and Marshall JF: The role of integrins in TGFβ activation in the tumour stroma. Cell Tissue Res 365: 657-673, 2016.
35. Golubovskaya V: Targeting FAK in human cancer: From finding to first clinical trials. Front Biosci (Landmark Ed) 19: 687-706, 2014.
36. Peixoto P, Etcheverry A, Aubry M, Missey A, Lachat C, Perrard J, Hendrick E, Delage-Mourroux R, Mosser J, Borg C, *et al*: EMT is associated with an epigenetic signature of ECM remodeling genes. Cell Death Dis 10: 205, 2019.
37. Cicchini C, Laudadio I, Citarella F, Corazzari M, Steindler C, Conigliaro A, Fantoni A, Amicone L and Tripodi M: TGFbeta-induced EMT requires focal adhesion kinase (FAK) signaling. Exp Cell Res 314: 143-152, 2008.
38. Attisano L and Wrana JL: Signal transduction by the TGF-beta superfamily. Science 296: 1646-1647, 2002.
39. Pardali E, Goumans MJ and Ten Dijke P: Signaling by members of the TGF-beta family in vascular morphogenesis and disease. Trends Cell Biol 20: 556-567, 2010.
40. Zavadil J and Böttinger EP: TGF-beta and epithelial-to-mesenchymal transitions. Oncogene 24: 5764-5774, 2005.
41. Hajra KM, Chen DY and Fearon ER: The SLUG zinc-finger protein represses E-cadherin in breast cancer. Cancer Res 62: 1613-1618, 2002.